Magnetic and crystal-field properties of dysprosium dihydrides and trihydrides from ^{161}Dy Mössbauer studies

J. M. Friedt*, G. K. Shenoy, B. D. Dunlap, D. G. Westlake, and A. T. Aldred
Argonne National Laboratory, Argonne, Illinois 60439
(Received 5 December 1978)

The saturation hyperfine magnetic field at the ^{161}Dy nucleus measured with the 26 keV Mössbauer resonance in $DyH_{2.00}$ identifies a Γ_7 crystal-field ground state for the Dy^{3+} atom. This state originates from a cubal surrounding of the Dy^{3+} atom by H^- atoms, in agreement with the hydridic model for rare-earth hydrides. An analysis of the hyperfine parameters and of the Schottky anomaly permits one to obtain the crystal-field parameters $W = 0.83 \pm 0.03$ K and $x = 0.24 \pm 0.02$, and the exchange field $H_{ex} = 26 \pm 5$ kOe. DyH_2 exhibits a long-range magnetic order at 3.3 K while between 3.3 and 6 K fairly complex short-range order is observed. A possible explanation for this behavior is provided. DyH_3 remains paramagnetic down to 1.6 K.

I. INTRODUCTION

The electronic and the magnetic properties of the rare-earth hydrides have been evaluated primarily from bulk measurements.[1] Recently, inelastic neutron scattering[2–4] and Mössbauer spectroscopy[5,6] have been used to probe the crystal field and the magnetic behavior of the rare-earth atoms in their hydrides. The present paper reports a Mössbauer investigation of stoichiometric dysprosium dihydride and trihydride using the 26 keV resonance in ^{161}Dy. A preliminary report on some of these results has already appeared.[7]

The rare-earth dihydrides are good electrical conductors. They crystallize in the cubic fluorite structure[8] with octahedral and tetrahedral sites that are occupied by rare-earth (RE) and hydrogen (H) atoms, respectively, as shown in Fig. 1. The additional octahedral sites which are available for the hydrogen atoms [$H(O_h)$ in Fig. 1] are nominally vacant in dihydrides, although there are reports to the contrary.[1,9] In the case of DyH_2, this point is discussed later in this paper.

Most of the rare-earth dihydrides show magnetic ordering at low temperatures. Magnetic susceptibility measurements[10] on DyH_2 indicate an antiferromagnetic ordering near 8 K. Our own susceptibility measurements show a broad deviation from the Curie-Weiss behavior below 6 K and no other anomaly down to 2 K. The specific-heat data[11] reveal a sharp λ anomaly at 3.3 K and a broad hump extending from 3.5 to 6 K (Fig. 2). A crystal-field level scheme in DyH_2 has been proposed from an analysis of the Schottky anomaly in the high-temperature specific-heat data.[12] Early Mössbauer measurements[13] on DyH_2 were restricted to room temperature, while a low-temperature study[14] showed fairly complex Dy^{3+} hyperfine spectra, perhaps due to uncertain stoichiometry of the sample.

In this paper we report Mössbauer measurements from 1.6 to 300 K on a carefully prepared sample of dysprosium dihydride with an atom ratio $H/Dy = 2.00 \pm 0.02$ and on a dysprosium trihydride sample with $H/Dy = 3.0 \pm 0.1$. We find the details of magnetic ordering at low temperatures and identify the crystalline electric-field (CEF) ground state in $DyH_{2.00}$. An estimate of the exchange field is also made. In $DyH_{3.0}$ the spectra are characteristic of paramagnetic relaxation phenomena down to 1.6 K.

One other aspect of considerable interest in rare-earth hydrides is in regard to the charge on the hydrogen ions. It has been shown earlier[5] that if the CEF ground state can be identified (from Mössbauer

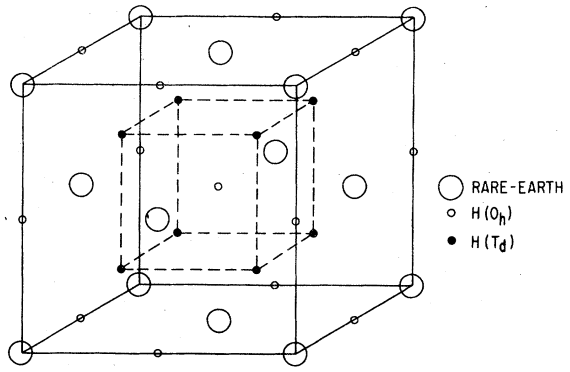

FIG. 1. Crystal structure of the rare-earth dihydrides showing the nominally filled tetrahedral and empty octahedral hydrogen sites.

studies), this will permit one to decide between the hydridic (H^-) and the protonic (H^+) description for hydrogen atoms in the lattice. This question will be considered in regard to DyH_2 in this paper.

II. EXPERIMENTAL

The ^{161}Dy Mössbauer spectra were measured with a source material which consisted of Gd-Dy F_3 with ^{160}Gd and ^{162}Dy enriched isotopes. The material was irradiated in a neutron flux of 6×10^{13} $cm^{-2}s^{-1}$ for a period of a week and was kept at room temperature during the measurements.

Dysprosium dihydride with an atom ratio $H/Dy = 2.00 \pm 0.02$ was produced by reaction of 99.9% pure Dy metal with purified hydrogen. The composition was determined from both volumetric and gravimetric analysis. The Debye-Scherrer diffraction patterns were in agreement with the literature data. Dysprosium trihydride with $H/Dy = 3.0 \pm 0.1$ was prepared in the same way and showed a characteristic hexagonal structure.[1]

The 26 keV γ rays were detected with a Kr-CO_2 proportional counter.[15] The counting gate was set over both the 26 keV γ-ray peak and the escape peak around 12 keV. The source was mounted on a electromechanical transducer to impart the needed Doppler shift in the resonance γ-ray energy and the spectrum was collected in a 1024 channel multiscaler operating in the time mode.

Typically the absorber thickness was 35 mg/cm^2 of natural Dy. The DyH_2 absorber at 300 K gave a resonance width of 6.5 mm/s against the above described source.

III. RESULTS

Dysprosium dihydride yielded a single line resonance spectrum between 300 and 6.5 K (Fig. 3). The linewidth varied from 6.5 mm/s at 300 K to 9.8 mm/s at 7 K. The broadening observed between these temperatures is primarily attributed to the absorber thickness effect. The isomer shift at 300 K is 0.70 ± 0.02 mm/s with respect to the source.

Below 7 K, the spectrum broadens sharply. In Fig. 4 we present the linewidth as a function of temperature down to 5 K. Between 5 and 3.3 K, the spectra reveal unresolved magnetic hyperfine patterns indicating the presence of a distribution of the magnetic hyperfine field (Fig. 3). The average hyperfine mag-

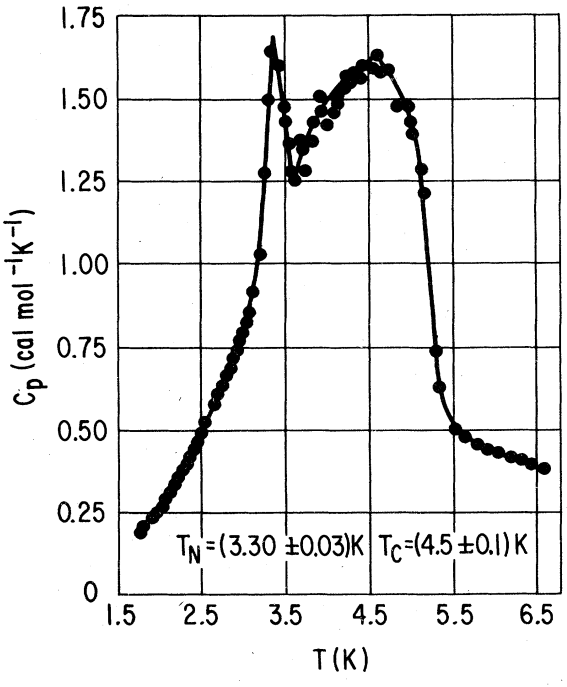

FIG. 2. Specific heat of DyH_2 in the vicinity of the magnetic ordering temperature (from Ref. 12).

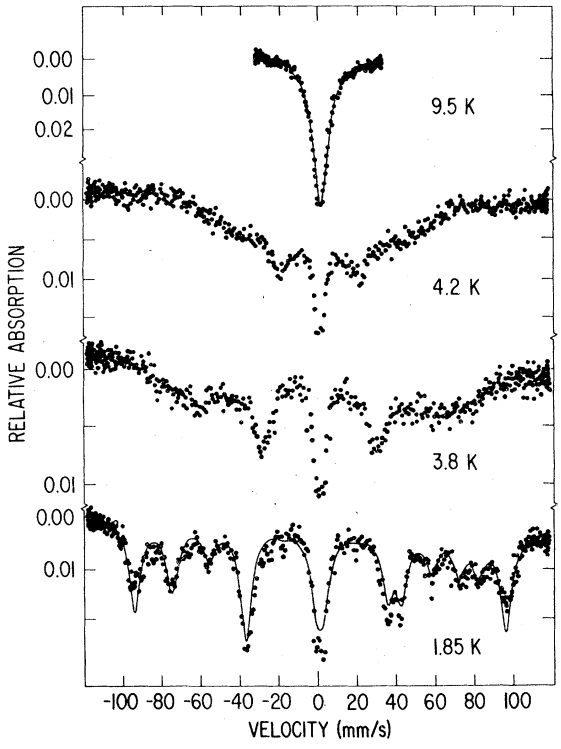

FIG. 3. ^{161}Dy Mössbauer spectra in $DyH_{2.00}$ at several temperatures.

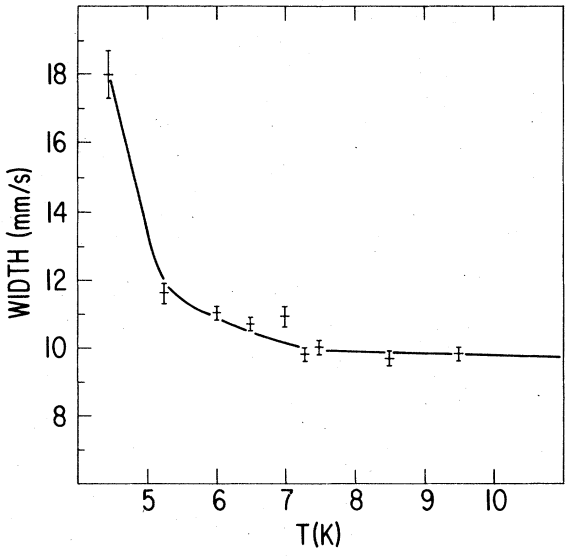

FIG. 4. Temperature dependence of the ^{161}Dy resonance linewidth obtained from single-line fits to the experimental data.

netic field increases gradually on lowering the temperature; typically the values are 1100 kOe at 4.3 K, 1500 kOe at 4.0 K, and 1800 kOe at 3.7 K. The distribution in the hyperfine magnetic field vanishes below 3.3 K and a sharp magnetic pattern characteristic of a single magnetic field is observed (Fig. 3). The hyperfine magnetic field at 1.6 K is $H_{\rm hf}=(2400\pm50)$ kOe and the quadrupole interaction is $e^2q_zQ=(185\pm20)$ MHz.

The resonance spectrum of DyH_3 at 300 K consists of a single resonance line with an isomer shift of (0.67 ± 0.05) mm/s relative to the source. The line broadens considerably at helium temperatures due to paramagnetic relaxation effects. There is no evidence for any magnetic ordering down to 1.6 K.

IV. DISCUSSION

A. Crystalline electric field and exchange field in DyH_2

The crystalline electric-field (CEF) Hamiltonian for a rare-earth atom occupying a cubic site has been treated in detail by Lea, Leask, and Wolf (LLW).[16] In the notation of LLW, the Hamiltonian is

$$\mathcal{H}_{CF}=\frac{Wx(O_4^0+5O_4^4)}{F(4)}+\frac{W(1-|x|)(O_6^0-21O_6^4)}{F(6)} . \quad (1)$$

The parameters W and x are defined by

$$\begin{aligned} Wx &= A_4\langle r^4\rangle\beta F(4) , \\ W(1-|x|) &= A_6\langle r^6\rangle\gamma F(6) , \end{aligned} \quad (2)$$

where A_4 and A_6 are the fourth- and sixth-order CEF parameters, $\langle r^4\rangle$ and $\langle r^6\rangle$ are $4f$ electron radial moments, β and γ are Steven's multiplicative factors, and $F(4)$ and $F(6)$ are 60 and 13 860, respectively, for the Dy^{3+} atom. The factors O_n^m in Eq. (1) are Steven's operators acting on J angular momentum states.

The cubic CEF will lift the sixteenfold degeneracy of the $^6H_{15/2}$ state of the Dy^{3+} atom, resulting in two doublets (Γ_6 and Γ_7) and three quartets (Γ_8^1, Γ_8^2, and Γ_8^3). One can attempt to predict the ground state from a simple point-charge model to calculate the CEF parameters.[16] Assuming[5] hydrogen to be H^- in DyH_2, we obtain $x=0.80$ and $W=0.51$ K. These parameters in Eq. (1) predict Γ_8^1 to be the ground state which is contrary to the experimental observation[17] of a Γ_7 ground state for the Dy^{3+} ion diluted in an YH_2 lattice. Indeed, for values of x less than 0.6, Γ_7 will be the ground state. On the other hand, if the hydrogens are protonic (H^+), the point-charge model predicts Γ_8^3 to be the ground state for values of x from 0 to 0.8. The significance of point-charge model is known to be limited to the prediction of the sign of x and W, which in DyH_2 depend on the sign of the charges on hydrogen atoms, whereas the absolute values are usually inaccurate.

In the magnetic state of the dihydride an exchange field H_{ex}, will act on the rare-earth atom. The energy of this interaction is obtained from

$$\mathcal{H}_m=-2\mu_B(g_J-1)\hat{J}\cdot\hat{H}_{ex} . \quad (3)$$

Depending on the direction of H_{ex}, the magnetic interaction $\mathcal{H}_m$ will have to be properly projected onto $\mathcal{H}_{CF}$ prior to diagonalizing the combined Hamiltonian. The influence of the exchange field will be mainly to mix the cubic CEF levels. The extent of this mixing will be determined by the relative strengths of the exchange and the crystal fields.

In the case of rare earths, the hyperfine interactions measured in the Mössbauer experiments are primarily determined by the nature of the CEF levels occupied at a given temperature. Given the energy eigenvalues, E_i (in K), and the CEF wave functions Γ_i, the hyperfine magnetic field produced by $4f$ electrons $H_{\rm hf}^{4f}$, and the quadrupole interaction e^2q_zQ, at any given temperature T are given by

$$H_{\rm hf}^{4f}=H_{Fl}\frac{\sum_i\langle\Gamma_i|J_z|\Gamma_i\rangle e^{-E_i/T}}{\sum_i Je^{-E_i/T}} , \quad (4)$$

and

$$e^2q_zQ = (e^2q_zQ)_{FI}\,\frac{\sum_i \langle\Gamma_i|3\hat{J}_z^2-\hat{J}^2|\Gamma_i\rangle e^{-E_i/T}}{\sum_i J(2J-1)e^{-E_i/T}} . \quad (5)$$

The value of free-ion hyperfine magnetic field H_{FI}^{4f}, for the Dy^{3+} ion is 6316 kOe and the quadrupole interaction $(e^2q_zQ)_{FI}$ for the free-ion is 3080 MHz (assuming $Q=2.35b$ for the ground state of ^{161}Dy and an inner shielding factor R, of 0.124).[18] In the absence of any exchange field, the above equations give for the Γ_7 ground state $H_{hf}^{4f}(\Gamma_7)=2390$ kOe and $e^2q_zQ(\Gamma_7)=0$. For a Γ_8 ground state one predicts an anisotropic field distribution of value higher than that of the Γ_7 doublet and a nonzero quadrupole interaction. The experimental value of 2400 ±50 kOe at 1.6 K is very close to the value characteristic of a Γ_7 ground state. The small quadrupole interaction of 185 ±20 MHz observed experimentally can arise by mixing of the higher CEF levels into the ground Γ_7 level by the exchange field.

We have searched for the best values of the parameters W, x, and H_{ex} in the Hamiltonian [Eqs. (1) and (3)] to account for both the hyperfine interaction parameters and the Schottky contribution to the specific heat. The wave function mixing by the exchange field, which is required to account for the finite quadrupole interaction measured in DyH_2, will necessarily increase the hyperfine field in comparison to the Γ_7 value. However, in a conductor like DyH_2 one predicts a conduction-electron contribution to add to the ion's own hyperfine field [Eq. (4)]. This has indeed been observed[5] in ErH_2; in this material, the conduction-electron contribution H_{hf}^{CE} to the hyperfine field at the Er^{3+} nucleus was concluded to be -200 kOe. H_{hf}^{CE} is proportional to the spin moment S, of the rare-earth ion and is negative for the second half-shell of the rare-earth ions

$$H_{hf}^{CE} \sim \langle S\rangle = (g_J-1)\langle J_z\rangle . \quad (6)$$

$\langle J_z\rangle$ is the effective angular momentum appropriate for the CEF configuration. Assuming identical band structures for ErH_2 and DyH_2, H_{hf}^{CE} for Dy^{3+} in DyH_2 can be scaled from the experimental value in ErH_2 using Eq. (6) to provide $H_{hf}^{CE}(Dy)=-450$ kOe. In Fig. 5 we present the calculated dependence of H_{hf}^{4f} and e^2q_zQ as a function of x for selected values of W and H_{ex} at 1.8 K. Correcting the experimental hyperfine field for the conduction-electron contribution, one observes good agreement between the calculated and the experimental hyperfine interactions for the following parameters in the Hamiltonian: $x=0.24$ ±0.02, $W=0.83$ ±0.03 K and $H_{ex}=26$ ±5 kOe. The value of the exchange field deduced here is based on the assumption that it is parallel to the [100] axis. The parameters deduced remain nearly the same if H_{ex} is along the [110] direction. However, a field along the [111] axis produces inconsistent hyperfine interaction parameters. The value of H_{ex} can be estimated within the framework of molecular-field theory.[19] In such an approximation

$$H_{ex}=\frac{3kT_c}{\mu}\,\frac{S}{S+1} , \quad (7)$$

where T_c is the transition temperature, μ is the magnetic moment, and $S=\frac{1}{2}$ for a Γ_7 ground state. Using the value $\mu=3.8\mu_B$ obtained from the measured hyperfine magnetic field, we find $H_{ex}=24$ kOe. The CEF scheme resulting from the above analysis is shown in Fig. 6.

The Schottky anomaly in the specific heat can be calculated using the expression

$$C_{sch}=\frac{R}{T^2}\,\frac{\left(\sum_i e^{-E_i/T}\right)\left(\sum_i E_i e^{E_i/T}\right)-\left(\sum_i E_i e^{-E_i/T}\right)^2}{\left(\sum_i e^{-\frac{E_i}{T}}\right)^2} , \quad (8)$$

where E_i represents the energy of the CEF level Γ_i, and R is the gas constant. In Fig. 7, experimental values[12] of C_{sch} are plotted. Equation (8) has been used to calculate C_{sch} for the crystal-field level scheme (of Fig. 6) and is shown as a solid line in Fig. 7; this describes the experimental result quite well.

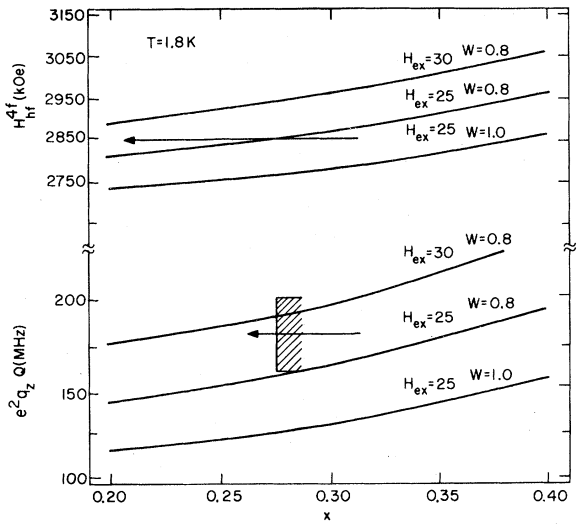

FIG. 5. Calculated hyperfine field (H_{hf}^{4f}) and quadrupole interaction as a function of the crystal-field parameters W and x, and of the exchange field H_{ex}. The experimental H_{hf}^{4f} (obtained after correcting for the conduction-electron contribution) and e^2q_zQ are indicated by the arrows.

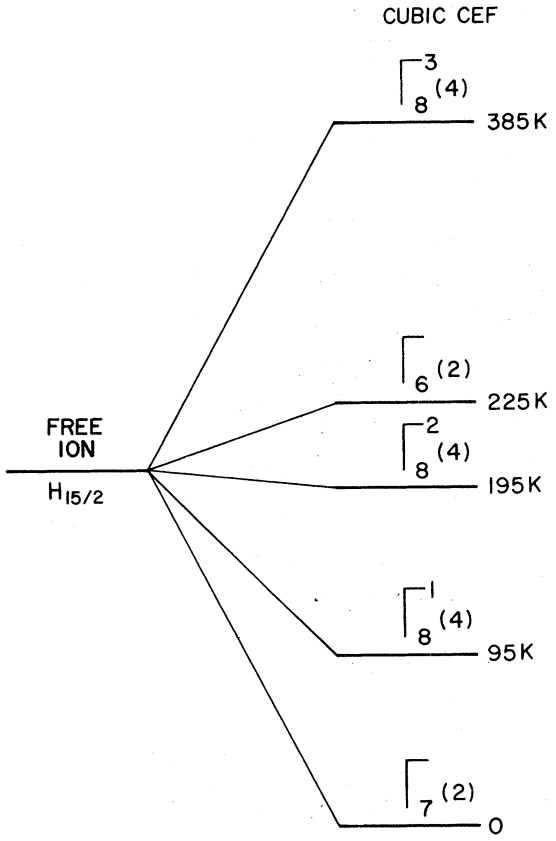

FIG. 6. Crystal-field level scheme for Dy^{3+} in DyH_2.

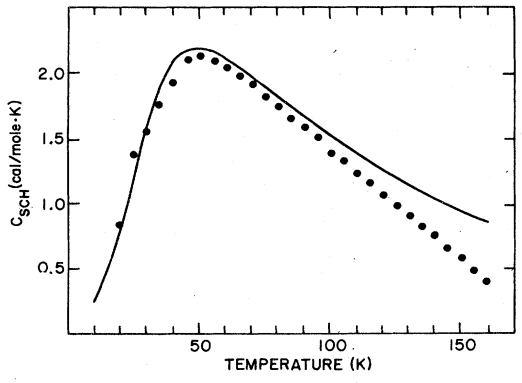

FIG. 7. Schottky contribution to the specific heat (Ref. 11) and calculated curve (solid line) from Eq. 8 with the CEF ordering as discussed in the text.

Although there may be some uncertainty in the experimental data points due to the necessity of correcting for the lattice and the magnetic contributions to the specific heat, the good agreement observed in the whole temperature range is a strong verification of the CEF level scheme deduced above.

When compared with predictions of the point-charge model, the deduction of a Γ_7 ground state in DyH_2 is in support of the hydridic model in which some of the electronic charge is transferred from the rare-earth atom to the hydrogen site. The negatively charged environment will then produce the CEF level scheme for the Dy^{3+} ion as shown in Fig. 6.

B. Details of the magnetic ordering in DyH_2

The observation of a well-defined magnetic hyperfine pattern below 3.3 K, together with a λ-type anomaly in the specific-heat curve[11] at this temperature, clearly shows the presence of long-range magnetic order in DyH_2. The absence of a pronounced anomaly in our powder susceptibility data at this temperature indicates this to be an antiferromagnetic ordering.

The behavior of DyH_2 between 3.3 and 6 K is rather curious. The specific-heat measurements (Fig. 2) show a broad bump with a maximum around 4.5 K. The possibility of this being a Schottky anomaly is ruled out by the results discussed in the last section. The sharp increase in the linewidth (Fig. 4) and a distribution in the hyperfine magnetic fields observed in the Mössbauer measurements definitely show this anomaly to be magnetic in origin. The average value of hyperfine magnetic field in this temperature range gradually increases on approaching 3.3 K; however, the value itself remains always less than that characteristic of a Γ_7 ground state. The details of the temperature dependence of the Mössbauer spectra rule out a strong distribution of ordering temperatures or paramagnetic relaxation effects. Also, this phase cannot originate from a one-dimensional or planar ordering in view of the isotropic nature of the Γ_7 ground state. Hence, it is suggested that this arises from magnetic, short-range order. Other rare-earth dihydrides exhibit a long tail in the specific-heat curve above T_N, characteristic of a short-range order.[20] However, the large anomaly observed in the specific heat of DyH_2 is unique.

This behavior can be qualitatively understood as follows: A small amount of disorder in hydrogen occupation between the tetrahedral and octahedral sites is probable, even in the most nearly stoichiometric compounds. This disorder will cause local distortions in the cubic CEF, and a commensurate deviation in the wave functions from the pure Γ_7 state for those Dy ions (relatively few in number for stoichiometric compounds) which are in the vicinity of the disor-

dered H atoms. Those ions having distorted ground states will always have a larger moment than those in the purely cubic sites. Because of the random distribution of the noncubic sites, there will be a distribution of local exchange fields acting on the other (cubically coordinated) Dy sites.

We consider the transition at 6 K to arise from an onset of short-range order nucleated by the larger moments on the noncubic sites. As a result the cubic sites are partially polarized by the local exchange fields. However, since there is a distribution in these exchange fields, there is a corresponding distribution in the degree of polarization and hence in the observed hyperfine fields. When the temperature is lowered to 3.3 K, normal long-range ordering occurs between the bulk of the ions (those in cubic sites) and the magnetic moments become fully polarized with the Γ_7 value. Since relatively few rare-earth atoms have distorted symmetry, their contribution to the Mössbauer spectrum is overwhelmed by that of the bulk of the material, and experimentally one sees a hyperfine splitting of the Γ_7 state only.

The sensitivity of exchange fields to slight hydrogen disorder implied above should strongly influence the magnetic properties of nonstoichiometric rare-earth hydrides. Indeed, our preliminary measurements confirm this expectation.

C. Paramagnetic relaxation in DyH_3

Although DyH_3 has a hexagonal structure when only the rare earths are considered, the location of the hydrogen atoms reduces the point symmetry of Dy^{3+} atoms to C_2. Thus one needs 15 CEF parameters to describe the detailed magnetic behavior. Observation of a single line at room temperature implies a fast spin relaxation with characteristic times shorter than 10^{-10} sec. Since DyH_3 is an insulator, the relaxation rate is expected to be slower at helium temperature. However, down to 1.6 K we have not observed a static hyperfine structure, precluding detailed analysis of the CEF in this case.

V. CONCLUSIONS

DyH_2 exhibits a long-range magnetic order below 3.3 K. The value of the hyperfine magnetic field and of the quadrupole interaction permits us to evaluate the CEF parameters and the exchange field. The results demonstrate that the hydrogen atoms carry a negative charge confirming the hydridic picture. The short-range order observed between 3.3 and 6 K is a manifestation of hydrogen disorder between the tetrahedral and the octahedral lattice sites and of the consequent distribution in the exchange fields. DyH_3 on the other hand shows only a paramagnetic behavior down to 1.6 K.

ACKNOWLEDGMENT

We would like to thank S. K. Sinha for many valuable discussions. This work was supported by the U.S. DOE.

---

*Permanent Address: Centre de Recherches Nucleaires, Strasbourg, France.

[1] *Gmelins Handbuch der Anorganische Chemie* (Springer, Berlin, 1974), Vol. 39, C1, p. 1.
[2] K. Knorr, B. E. F. Fender, and W. Drexel, Z. Phys. B 30, 265 (1978).
[3] D. G. Hunt and D. K. Ross, J. Less Common Metals 45, 229 (1976).
[4] T. Brun and S. K. Sinha (private communication).
[5] G. K. Shenoy, B. D. Dunlap, D. G. Westlake, and A. E. Dwight, Phys. Rev. B 14, 41 (1976).
[6] B. Suits, G. K. Shenoy, B. D. Dunlap, and D. G. Westlake, J. Magn. Magn. Mater. 5, 344 (1977).
[7] G. K. Shenoy, J. M. Friedt, B. D. Dunlap, and D. G. Westlake, Phys. Lett. A 67, 241 (1978).
[8] R. N. R. Mullford and C. E. Holley, J. Phys. Chem. 59, 1222 (1955).
[9] P. Vorderwisch and S. Hautecler, Phys. Status Solidi B 66, 595 (1974).
[10] Y. Kubota and W. E. Wallace, J. Chem. Phys. 39, 1285 (1963).
[11] Z. Bieganski, J. Opyrchal, and M. Drulis, Phys. Status Solidi A 28, 217 (1975).
[12] Z. Bieganski and J. Opyrchal, Bull. Acad. Polonaise. Sci. 20, 775 (1972).
[13] T. P. Abeles, W. G. Bos and P. J. Ouseph, J. Phys. Chem. Solids 30, 2159 (1969).
[14] J. Hess, E. R. Bauminger, A. Mustachi, I. Nowik, and S. Ofer, Phys. Lett. A 37, 185 (1971).
[15] D. W. Forester and W. A. Ferrando, Nucl. Inst. Methods 108, 599 (1973).
[16] K. R. Lea, M. J. M. Leask and W. P. Wolf, J. Phys. Chem. Solids 23, 1381 (1962).
[17] J. Stöhr and J. D. Cashion Phys. Rev. B 12, 4805 (1975).
[18] B. D. Dunlap, in *Mössbauer Effect Methodology,* edited by I. J. Gruverman (Plenum, New York, 1971), Vol. 7, p. 123.
[19] J. S. Smart, *Effective Field Theories of Magnetism* (W. B. Saunders, Philadelphia, 1966), p. 24.
[20] Z. Bieganski and B. Stalinski, J. Less Common Metals 49, 421 (1976).